LIGHT STIMULATED NANOCOMPOSITE SYNTHESIS AS A MODEL OF PHOTOINDUCED PHENOMENA IN INORGANIC THIN FILMS

N. Starbov[*], K. Starbova

Central Laboratory of Photoprocesses "Acad. J. Malinowski" Bulgarian Academy of Sciences 1113 Sofia, Bulgaria

Dedicated to our lovely teacher Acad. J. Malinovski

The outlines of present talk are photoinduced effects in light sensitive binary chalcogenides and refractory oxides reviewed on applying the concept for synthesis of composite materials. Generation of various nanostructured phases in the light absorbing media under specific irradiation conditions is exemplified by the formation of nanoparticles(voids)/matrix, nanocrystallite/amorphous and multi component composites. Evolution of a great variety phase compositions and morphologies and related properties which are not possible to realize with the unirradiated materials are demonstrated. The singnificance of the approach for the development of novel functional materials is discussed. The importance of knowledge on the fundamentals of the photographic process in classical silver halide materials for the proposed concept is emphasized.

1. Introduction

Solid state photosensitive binary compounds are object of a constant interest in material science for almost two centuries. In that field of research the intense studies on fundamentals of light/matter interaction usually follow the discovery of a proper photo-induced effect. Important results and related conclusions are restricted, with some exceptions, to the material of interest or mostly to the corresponding class it belongs to. Different scientific terms are given to photo stimulated effects of same origin for various compound families. Single properties are explained as a consequence of unique processes occurred after the light absorption. At the same time attempts for drawing general conclusions on the similarity of the operation mechanisms at atomic or molecular scale are often subjected to criticism and soon forgotten.

Albert Einstein formulated the basic relations of the photoeffect 100 years ago. For that reason we find the conference timing and symbolic. Because, it is the internal photoeffect that contributes to the most photoinduced phenomena in condensed matter. Upon photon absorption free charge carriers, electrons and holes, with kinetic energy (E) are generated, within the lattice of dielectrics and semiconductors

$$E = \hbar\omega - E_g \qquad (1)$$

when the photon energy ($\hbar\omega$) exceeds corresponding energy band gap, E_g ($\hbar\omega \geq E_g$).

On irradiation of silver halides (AgX) with actinic light, generation of electrons in the conduction band and holes in the valence band takes place. Photoconductivity measurements evidence a low recombination rate of photogenerated charge carriers [1]. As a result photoinduced decomposition of AgX takes place leading to separation of visible, photolytic Ag and corresponding halogen [2]. The conventional black/white photography is based on the very early stages of

---

[*] Corresponding author: ilka@clf.bas.bg

photolysis and therefore to the formation of nano-sized silver clusters, called latent image [3]. The later is further intensified to visible image during the development that is the last l stage of the conventional photographic process. Studies on arrested, initial development stages reveal a small number developed centers and related latent image specks in silver halide emulsion grains. That is explained by the operation of an unique concentration mechanism whose basic principles are formulate in 1938 by Gurney and Mott [4]. They postulate an occurrence of two stage process. During the first stage photo-generated electrons are captured by active nanosized impurity centers at AgX surface or volume structure defects. In the second stage a neutralization of the trapped charge proceeds, via Coulomb attractive forces, by silver ion interstitials (Ag^+) which are intrinsic equilibrium lattice defects. Further the Gurney and Mott scheme envisages growth of silver clusters to developable size via consecutive electron trapping and charge neutralization processes. In the final step, during the photographic development a huge amplification (10^5-10^9 times) takes place leading to the formation of visible silver image in specific solutions called chemical or physical developers, the latter representing silver electroless plating baths.

In a series elegant model quantitative investigations on AgBr single crystals Malinowski and co-workers determine the basic parameters of the photo-generated holes [5-7]. On this basis the mechanism for photo-induced changes in AgX is complemented, thus giving birth to the "symmetric scheme" of the primary photographic process [8]. An important element of that scheme is the presence of channel for neutralization of photo-generated holes by silver ion vacancies, the other equilibrium lattice defects, within the volume and their transport to the AgX surface where they behave as a free halogen which escapes in the ambient. Thus, the surface acts as a pump and all generated holes release the crystal via diffusion due to the concentration gradient within the crystal volume. The discovery of the bleaching, oxidizing ability of the corresponding halogens on the surface can be also regarded as an important contribution to the mechanism of the photographic process in positive AgX emulsions and it stimulated the development of novel AgBr thin film based positive materials [9]. On the basis of computer modeling experiments [10] and model investigations in AgBr thin films [11] it is further demonstrated that the formation of developable silver nanosized clusters can be successfully interpreted applying the concepts for spontaneous heterogeneous nucleation of single atoms generated by Gurney&Mott principle. As a consequence of that generalized model the operation of concentration mechanism during latent image formation is already not necessary and the photographic process in AgX should be deleted from the list of unique photo-induced phenomena.

In terms of the contemporary material science a photo-induced "synthesis" of a metal matrix nano-composite (AgX matrix and Ag clusters) takes place upon light absorption in AgX. By definition the composite is a combination of at least two constituents differing in composition and structure which retain their identities, exhibit an interface between each other, do not dissolve or merge and act in concert.

The following question arises. Is it reasonable to apply the knowledge and experience of silver halide photography for elucidation the fundamentals of light/matter interaction of other photosensitive binary compounds?

Crystalline semiconductors whose energy band gaps are relatively close to those of AgX as TiO_2 and SnO are between the first drawing attention. The efforts for autocatalytic amplification of photo-induced changes in by processing in electroless plating baths meet with success and favor the development of novel non-silver negative materials [12].

Later, a bold attempt appears, recently known as bond-breaking model, for explaining the mechanism of photo-structural changes (understand photographic process) in As chalcogenides representing amorphous semiconductors [13]. Making an analogy with AgX the model envisages the occurrence of light induced photo-decomposition of chalcogenides that is accompanied by nucleation and growth of As clusters. Subsequently, reliable experimental evidence supporting the above hypothesis are published [14, 15]. Recently, however, the most popular model for the photostructural changes in arsenic chalcogenides is that predicting polymerization of molecular spieces [16].

In the present paper the results from long term experiments on photosensitive binary compounds of amorphous chalcogenides and refractory oxides are summarized and interpreted applying the concept for light stimulated separation of a new phase of own metal and tailoring of composite material.

2. Experimental

The samples studied represented thin films of chalcogenides As_2S_3 and $GeSe_3$ and refractory oxides of ZrO_2, Al_2O_3 and TiO_2. The first were obtained by thermal evaporation (Joule effect) of high purity chalcogenides at a mean deposition rate of 0.1 nm/s on silicate glass plates coated with adhesive polymer film. The refractory oxides were obtained either under high vacuum conditions or from solutions. In the first case samples were deposited via e-gun evaporation of high purity targets on pre-cleaned glass or quartz plates at a mean deposition rate of 0.2 nm/s. The sol-gel ZrO_2, Al_2O_3 and TiO_2 thin film samples were prepared via multiple spin coating of appr. 50 nm thick single films from stabilized isopropanol solutions of corresponding isopropoxide precursors followed by 20 minutes non-isothermal heating at 120 ^{o}C or for titania films at 360°C. Except for TiO_2 all as coated films were X-ray amorphous.

The irradiation of chalcogenide films were performed by means of 200 W Hg lamp having 20 mW/cm^2 intensity at the specimen surface. The thin films of refractory materials were photo-thermally processed by means of excimer (KrF*, $\lambda = 248$ nm, $\tau = 20$ ns) and (ArF*, $\lambda = 193$ nm, $\tau = 20$ ns) pulsed laser irradiations with single shots or in repetitive mode in the presence of beam homogenizer, the energy density and the pulse number being the laser parameters varied.

Two stage decoration procedure was used for visualization of photo-induced changes in chalcogenide films under investigation. These are revealing of the volume changes in specific chemical solutions [17] and further amplification in physical developer which in fact is an electroless silver bath [18]. The laser induced photo-thermal transformations in refractory oxide films were intensified in low speed alkaline Mc Dermit commercial Ni or Cu electroless plating baths [19].

In order to characterize the photo-structural changes in the films studied a combination of analytical and imaging methods as optical densitometry, optical spectrophotometry, scanning (SEM) and transmission (TEM) electron imaging, X-ray and electron diffraction phase analysis.

3. Results and discussion

Results from typical photolytic experiment after heavy illumination with bandgap light are shown on the scanning electron micrographs on Fig. 1 for 100 nm thick As_2S_3 (a) and $GeSe_3$ films (b) The optical micrograph of visible photolytic Ag in 400 nm thick AgBr thin films on Fig.1c is given for comparison. It is clearly seen the separation of crystalline phase of As_2O_3 (a) GeO (b) and Ag as confirmed by corresponding XRD phase analysis. Obviously, in parallel to As-S and Ge-Se bond breaking oxygen and/or moisture assisted processes take place in chalcogenides during prolonged exposures. What happens on decreasing the irradiation dose is not clear since the photostructural changes become beyond the resolution or sensitivity limit of all known imaging and great number analytical techniques. In studying these photoinduced effects in chalcogenide thin films the optical spectrophotometry preserves, during several decades, the privilege to have a priority over the other analytical methods. The major contributions in the field are related to photodarkening and absorption edge red shift [20] or photobleaching and absorption edge blue shift [21], as well as accompanying change in the physical and chemical properties in arsenic or germanium chalcogenides correspondingly.

Fig. 1. SEM micrographs (a,b) of 100 nm thick As_2S_3 (a) and $GeSe_3$ (b) films after heavy UV irradiation. Optical micrograph of photolytic Ag (black) in 400 nm thick AgBr film (c).

The research on silver halides is plenty of important optical parameters that are related to almost all photoinduced effects [22]. Nevertheless, we dared to perform simple measurements of the optical transmission change in 400 nm thick AgBr films after prolonged, print out exposure with actinic light. The recorded transmission spectra are displayed on Fig. 2.
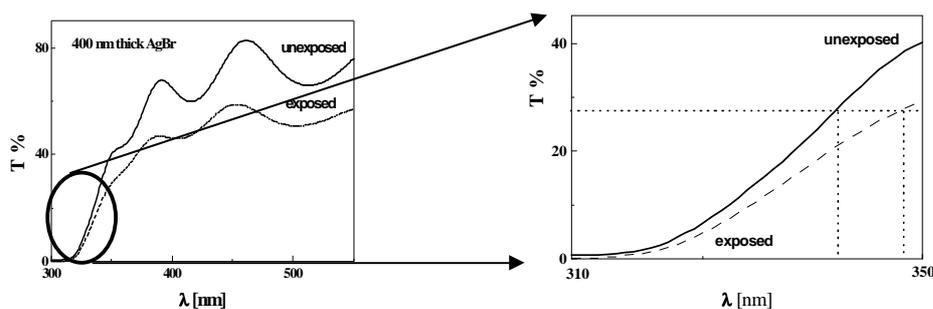

Fig. 2. Optical transmission spectra of 400 nm thick AgBr thin films: unexposed and exposed for 40 min. with Hg lamp a light intensity at the sample surface of 20 mJ/cm^2.

As could be expected, as a result light absorption a photo-darkening in AgBr takes place that is accompanied by the absorption edge shift to lower energy, similarly to the same effect in As chalcogenides. This first milestone reveal a possibility to apply classical for AgX processing autocatalytic amplification in order to study the photodarkening in arsenic sulfide and germanium selenide thin films. Fig. 3 presents optical transmission micrographs of micrometer details (a) reproduced in 100 nm thick As_2S_3 films via UV irradiation through a Cr mask (b) and a sequence of wet chemical procedures the last being electroless silver plating [23]. As a result visible, silver image is bult up. Fig. 5 shows high magnification images of copied silver details resolving submicron line in $GeSe_3$ (a) and As_2S_3 (b) films. Therefore, similarly to arsenic sulfide $GeSe_3$ films exhibit a negative photoresponse that can be visualised under appropriate irradiation and processing conditions. On this basis a more general conclusion could be drawn. Developable clusters are formed within the volume of as deposited unannealed chalcogenide films during their irreversible photodarkening. That is similar to the latent image formation in AgX. At first side this modest result has a substantial consequence. It reveals possibility to apply the quantitative apparatus of AgX photography for evaluation of the photoresponse in chalcogenide films studied.
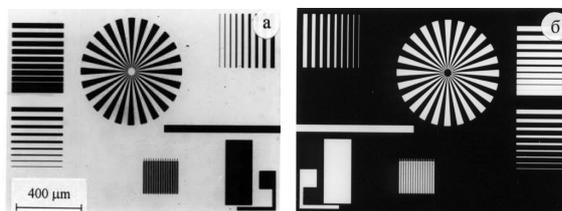

Fig. 3. Optical transmission micro-graphs of negative silver image of micron and submicron details (a) after contact copying of Cr mask (b) and photographic processing of As_2S_3 films.

On the basis of simple optical density measurements after irradiation through specific optical step wedge and photographic processing (Fig. 4), characteristic curves displaying the relation between developed density (D) and light energy (H=It), can be drawn (Fig. 6). Important photographic parameters can be estimated from these curves. These are maximal and fog density (D_{max}, D_{min}) determined by the number of light generated and fog (background) clusters respectively, contrast coefficient (γ) and sensitivity. The latter is related to the curve position with respect to the exposure axis and is evaluated from the linear part of the curve. Typical D/lgH curves obtained according to the scheme on Fig. 4 and 100 nm thick As_2S_3 films as light sensitive medium are

displayed on Fig. 7, the irradiation time increasing from 1 to 5, keeping constant the light intensity, precipitation rate and electroless plating processing conditions. Obviously, at low irradiation doses the amorphous As_2S_3 films studied exhibit a negative photoresponse that could be visualized by more or less standard photographic processing. It is clearly seen D_{max} decrease with increasing the irradiation dose. Therefore in parallel to the formation a of developable clusters a competitive process takes place leading to a decrease of their numbers and/or size. Having in mind the separation of As_2O_3 at heavy exposures (Fig. 1a) a partial oxidation and thus a loss of developability of arsenic clusters in the advanced irradiation stages could be reasonably assumed. Further, the basic photographic parameters of the established negative photoresponse as dependent on the As/S ratio were evaluated.

hν
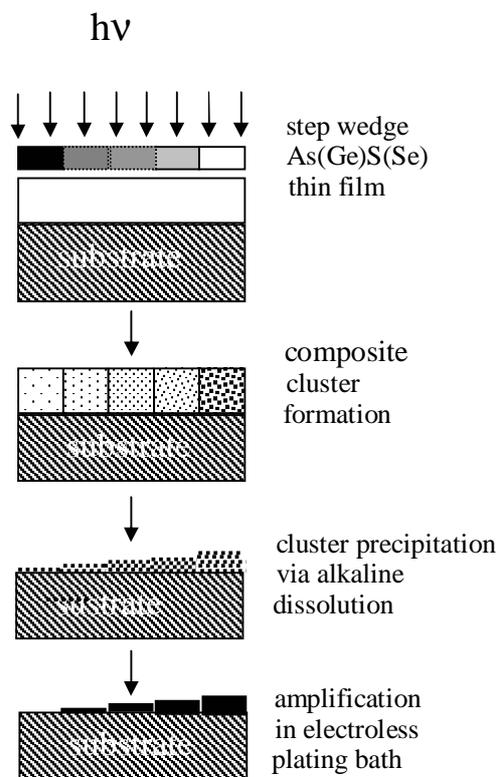
Fig. 4. Stages of visible image formation via actinic irradiation and photographic processing.
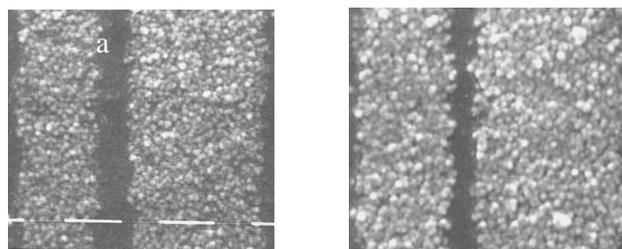

Fig. 5. High magnification images of silver submicron detail reproduced in 100 nm thick GeSe₃ (a) and (b) As₂S₃ films.
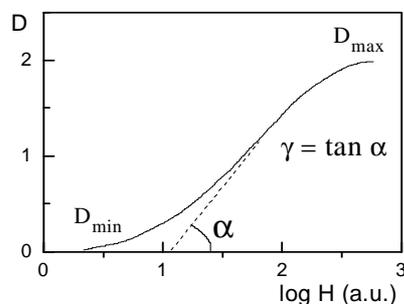
Fig. 6. Characteristic curve: developed optical density (D) versus exposure (H=I.t).

As seen from Fig. 8 the measured D_{max} values are sensitive function to As-S content being maximal for As_2S_3 films. Obviously, the efficiency and stability of developable As cluster are greatest in As-S films with highest As content studied. Except for increasing As content the same trend on D_{max} value have been obtained at low temperature exposures and photographic processing [24] thus confirming classical results on photodarkening effect at liquid nitrogen [9].
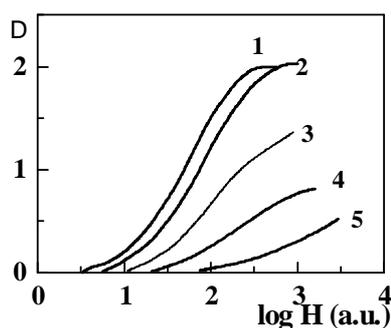
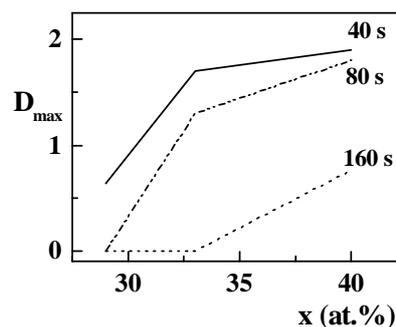Fig. 7. D/lgH curves on increasing exposure time (1→5) of 100 nm thick As_2S_3 films.

Fig. 8. Plot of Dmax versus As content for different irradiation times.

Here, the higher efficiency of the internal latent image, i.e. Ag cluster formation in AgBr emulsions under irradiations at liquid air should be reminded [25]. Moreover, in both cases the induction period of the development is found to become longer with decreasing the exposure temperature thus evidencing a dispersity increase, respectively size decrease of As or Ag cluster formed. Studies on the nature of the photographic sensitivity unambiguously demonstrated that the photo-induced changes of AgX can be modeled by vapor deposited nanosized silver clusters [26]. The latter are able to initiate further deposition of silver from electroless plating baths [18] as well as to be oxidized to AgX by the corresponding halogen. It was f ound that vapor deposited arsenic metal on As_2S_3 in the nanosized thickness range also catalyses Ag deposition from such baths. As seen from Fig. 9 increasing the light intensity the initially maximal developed density is reduced and a typical for positive materials characteristic curve is obtained. On this basis it is reasonable to conclude that during the irradiation the arsenic clusters are destroyed by the mobile photo-generated holes which have measurable mobilities and lifetime especially in the chalcogenide glasses [27]. It seems therefore, that under the absorption of actinic light a composite is tailored that is comprised of chalcogenide phase matrix and nano-structured phase of dipersed own metal. Because of the high chemical reactivity the latter could be visualized by well developed and powerful photographic processing routes.
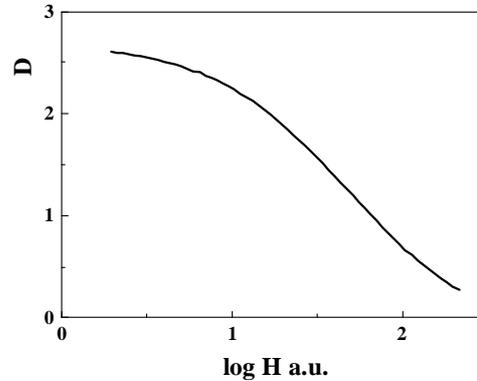
Fig. 9. Characteristic curve of As/As$_2$S$_3$ thin film system after a step wedge UV irradiation
and electroless silver plating.

Oxide ceramic are also an important object of applied and fundamental interest. To this
contribute combinations of unique thermal, electrical, chemical, mechanical and other functional
properties [28] offering possibilities for development of various functional materials in thin film
form. Both vacuum and purely chemical technologies are usually applied for large scale production
of ceramic thin films. Often an additional high temperature treatment of as deposited films is
necessary in order to prepare crystalline films with proper phase composition. Since the majority of
oxide ceramics are wide band gap materials for special purposes this processing could be performed
applying excimer pulsed lasers as modification tool. Under specific laser irradiation conditions
below the ablation threshold the ceramic thin films undergo various photo-thermally processes as
melting/solidification, photolysis, pyrolysis etc. resulting in well controlled-ordered products
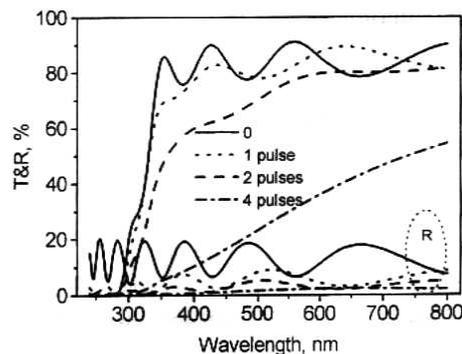[29,30].

Fig. 10. Optical transmission (T) and specular reflection (R) spectra of 800 nm thick ZrO$_2$
films, as deposited and excimer laser irradiated at pulse fluence 0.75 J/cm^2 upon
increasing the pulse number.

What for photo-induced changes take place after KrF* excimer pulsed laser irradiation of
zirconia thin films? As demonstrated by the T-spectra on Fig. 10, the optical absorption edge seems
to be shifted toward lower energies upon multiple irradiations at constant laser fluence. Since the
changes on R-spectra are relatively smaller as compared to T-spectra the contribution of the light
scattering for that shift could be neglected. Similar trend of the recorded T & R spectra exhibit ZrO$_2$
thin samples excimer laser irradiated on increasing the laser fluence at constant pulse number. On
this basis it could be assumed that excimer laser absorption increases between consecutive pulses as
displayed by the normalized absorbance (A) spectra of single shot irradiated ZrO$_2$ thin films as a
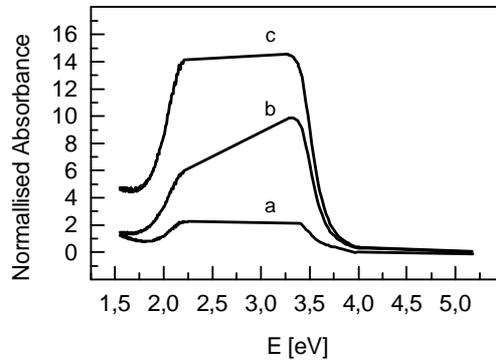function of laser fluence.

Fig. 11. Normalized optical absorbance [$(A_{irradiated} - A_{virgin})/ A_{virgin}$] spectra single shot irradiated 800 nm thick ZrO_2 films upon increasing pulse fluence from 0.75 (a) to 1.25 J/cm^2 (c).

Analogous optical transmission and reflection spectra were also recorded from e-beam deposited alumina and titania thin films as well as from multilayered sol-gel zirconia and titania subjected to excimer laser modification below the ablation threshold. Fig. 11 manifests examples of 1000 nm thick vapour deposited on quarz substrate alumina (a) and 700 nm thick sol-gel titania films single shot irradiated upon increasing pulse laser fluence by means of ArF*(a) and KrF* (b) excimer lasers. Photodarkening effect and accompanying optical absorption edge shift to low energy are clearly seen. The decrease of the specular reflection as a result of laser modification albeit relatively small compared to that of the transmission give an indication for changes of the surface relief. Surface morphologies of 700 nm thick sol-gel TiO_2 film before (a) and after excimer (KrF*) laser processing with different pulse number are shown on Fig. 13. As seen from the figure as a result of laser processing the fine grained surface of the nonirradiated sample (a) becomes rough, bubbles (b) and pores (c) being specific morphological features. Obviously, the latter are result of fast melting/solidification processes due to the heat release during the light absorption.
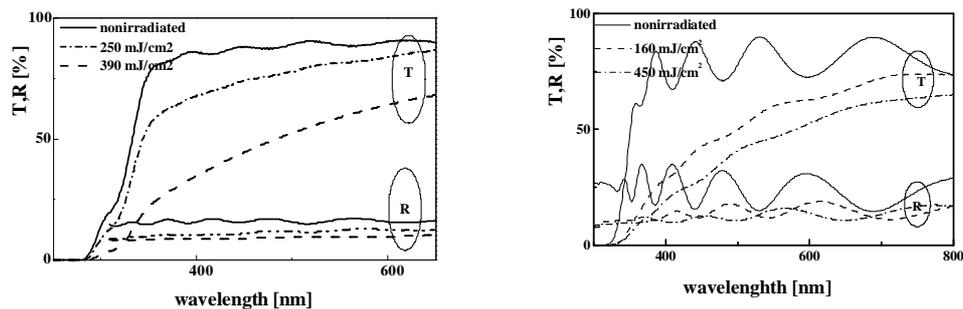

Fig. 12. Optical transmission (T) and specular reflection (R) spectra of 1000 nm thick e-gun deposited Al_2O_3 films (a), and 700 nm thick sol-gel TiO_2 films as deposited and excimer laser irradiated upon increasing the pulse fluence.
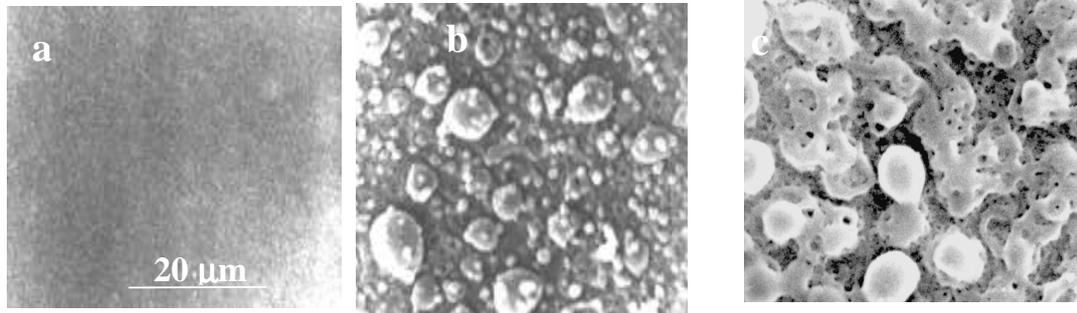
Fig. 13. Scanning electron micrographs of 700 nm thick sol-gel TiO_2: nonirradiated (a) and excimer (KrF*) laser irradiated at pulse fluence 300 mJ/cm^2 with single shot (b) and 5 pulses at 1Hz repetitive rate - (c).

As seen from the scanning electron micrographs on Fig. 14 an evolution of a high specific surface area in vapor deposited zirconia films is developed after multiple excimer laser irradiation. It should be noted that different degree of surface roughening was observed in all excimer laser processed vapor deposited or sol-gel films studied. Further, X-ray and electron diffraction analysis were performed in order to study the phase composition of laser modified films. Fig. 15 shows transmission electron micrograph and corresponding SAED pattern of single shot irradiated ZrO_2 film. The results from electron imaging and diffraction analysis evidence a composite structure that comprises of nanostructured amorphous, orthorhombic and monoclinic ZrO_2 together with hexagonal ω–Zr [29]. Besides, under specific laser irradiation conditions the phase composition could be changed in a controlled way to metastable cubic ZrO_2, ω–Zr being always a phase component of the composite. Similarly, high temperature γ-Al_2O_3 phase was found to co-exist with amorphous alumina in laser modified vapor deposited Al_2O_3 thin samples [30].
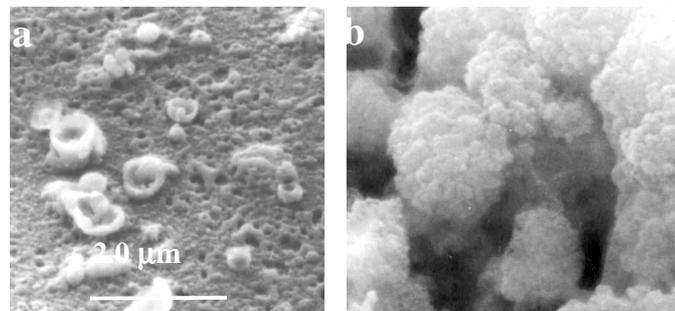

Fig. 14. Scanning electron micrographs of 650 nm thick e-gun deposited ZrO_2 excimer (KrF*) laser irradiated at pulse fluence 800 mJ/cm^2 with 3 pulses (a) and 100 pulses at 1Hz repetitive rate - (b).
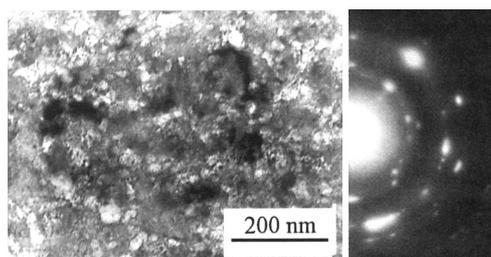

Fig. 15. Transmission electron micrograph (extraction replica, bright field mode) and SAED pattern of single shot (750 mJ/cm^2) irradiated 800 nm thick ZrO_2 film.

The initially amorphous/anatase composite structure of laser processed sol-gel TiO_2 is preserved on X-ray diffraction scale, an increase of crystallinity degree is observed [31]. As demonstrated by the high magnification (bright and dark field mode) transmission electron micrographs of mulitiple (5 pulses, 1Hz, 300 mJ/cm^2) irradiated 1200 nm thick sol-gel TiO_2 samples on Fig. 16, the laser transformed near surface region has also an amorphous/crystalline nano-composite structure [32].
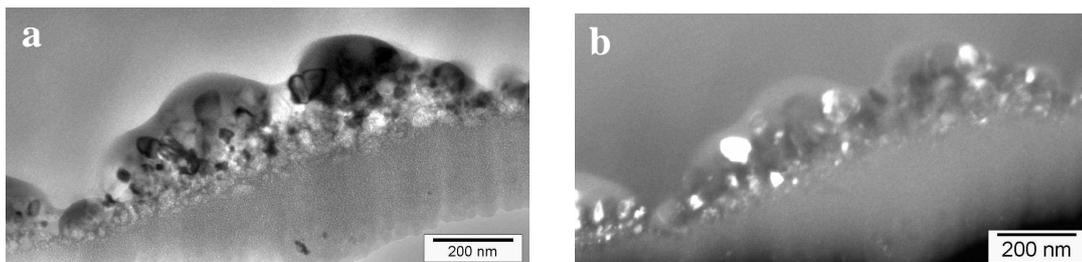

Fig. 16. Transmission electron micrographs of 700 nm thick sol-gel TiO_2 excimer (KrF*) laser irradiated at pulse fluence 300 mJ/cm^2 with 5 pulses (1Hz repetitive rate): bright field mode (a) and dark field mode (b).

It might be noted the ability of laser processed bulk ceramics to be activated with respect to metal plating. This technique provides electroless metal deposition in laser processed regions with a high selectivity. Similarly, it was established that excimer laser processed thin zirconia and alumina films within specific range of pulse laser parameters promote deposition Ni and Cu from alkaline electroless plating baths as demonstrated on Fig. 17 for sol-gel ZrO_2 film on stainless steel substrate and Ni coating. Most probably nanoclusters of ω–Zr hexagonal phase act as active centers in the initial stages of electroless plating that continues auto-catalytically in advanced stages. At present, γ-Al_2O_3 phase [33] or nanostructured aluminum phase [34] are believed to be responsible for the laser enhanced plating of alumina bulk ceramics. In our opinion, the contribution of both phases during the initial stages of electroless metal deposition have to be considered.
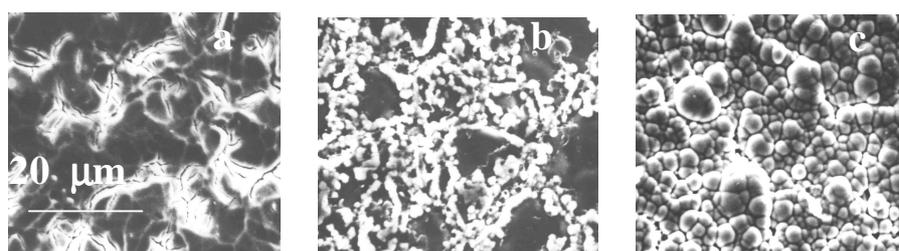

Fig. 17. Scanning electron micrographs of multilayered sol-gel ZrO_2 film: unexposed (a), single shot (1.4 J/cm^2) irradiated (b) and single shot irradiated and 60 min. electroless Ni plated (c).

In summary, it might be concluded that the modification of thin ceramic films by means of excimer pulsed laser irradiation results in light induced synthesis of metal ceramic composites. The phase composition of the latter could be varied in a wide range as depending on pulse laser parameter.

4. Conclusions

In the present paper an attempt was made to qualify the photostimulated effects in some binary compound as a light induced synthesis of nanocomposites. The basic considerations originate from the theory of the photographic process in classical silver halide materials having 170 years experience. Without going into details in the mechanism of light matter/interaction and the defect

structure, separation of a phase of own metal within the volume of different binary compounds is demonstrated to be one "binding" element of the corresponding light- or photo-thermal response. The newly formed phase initiates metal electroless plating regardless the structure and composition of thin film matrix it originates from and is therefore nanostructured and in a highly dispersed state. Applying lasers as a tool for photo-thermal synthesis a great variety of multicomponent composites are possible to be produced thus revealing routes for design of novel functional materials.

Acknowledgements

References

[1] W. Lehfeldt, Nachr. Ges. Wiss. Goettingen, Kl., **1**, 171 (1935); K. Hecht, Z. Physik, **77**, 171 (1932).
[2] "The theory of the photographic process", Ed. C. E. Keneth Mees, Revised Edition, The Macmilan Company, 1954, p.124.
[3] ibid., p.503.
[4] R. W. Gurney, N. F. Mott Proc. Roy. Soc. (London) Ser. A, **164**, 151 (1938).
[5] V. Platikanova, J. Malinowski, phys. stat. sol. **14**, 205 (1966).
[6] A. Buroff, J. Malinowski, phys. stat. sol. **26,** 267 (1968).
[7] M. Georgiev, J. Malinowski, phys. stat. sol. **28,** 725 (1968).
[8] J. Malinowski, J. Phot. Sci. **16,** 57 (1968).
[9] B. Mednikarov, Ph.D Thesis, "Preparation and properties of thin evaporated AgBr Layers", Sofia, 1984.
[10] N. Malinowski, J. Malinowski, J. Imag. Sci. **29**, 105 (1985).
[11] K. Starbova, V. Platikanova, Phot. Sci. Eng. **23**, 107 (1979).
[12] U.S. Patent 3409429, cl.96-27); Avtorskoe svidetelstvo 593179, M.Kl.2. G03 C 1/72, SSSR, in Russian; Perspectivi i vozmojnosti neserebriannoi photographii, Ed. A. L. Kartuzhanskii, Izd. Himia (in Russian), 1988, p.24).
[13] J. S. Berkes, S. W. Ing, W. J. Hillegas, J. Appl. Phys. **42**, 4908 (1971).
[14] Ka. Tanaka, M. Kikuchi, Solid State Commun. **11**, 1311 (1972).
[15] M. Frumar, A. Firth, A. E. Owen, Phil. Mag. **B 5**, 463 (1984).
[16] J. P. DeNeufville, S. C. Moss, S. R. Ovshinsky, J. Non-Cryst. Solids **13**, 191 (1973/1974).
[17] I. Konstantinov, B. Mednikarov, M. Sachatchieva, A. Burov, US Patent 4 499 173 (1985).
[18] J. P. Archambault, N. H. Nashua, W. S. Holmes, US Patent 3 672 899 (1972).
[19] Mc Dermit Elnic 101.
[20] J. P. DeNeufville, in Optical Properties of Solids- New Developments (Ed. B. O. Seraphin) North Holland, Amsterdam 1975, p. 437.
[21] L. Tichy, L. Ticha, K. Handlir, K. Jurek, Phil. Mag. Lett. **58(5)**, 233 (1988).
[22] "The theory of the photographic process", Ed. T. H. James, The Macmilan Company, Third Edition, (in Russian), 1973, Chapter 1, p. 30.
[23] J. Dikova, N. Starbov, K. Starbova, J. Non-Crystall. Sol. **167** 50 (1994).
[24] J. Dikova, B. Tomerova, "Effect of Low Temperature Exposure on the Photographic Process , Proc. of 10th Int. School on Cond. Matt. Phys.,"Thin Film Materials and Devices – Developments in Science and Technology", Eds. J. Marshall, N. Kirov and A. Vavrek, p.497, (1999).
[25] W. F. Berg, A. Marriage, G. W. W. Stevens, Phot. J. **81,** 413 (1941) Comm.794H.
[26] J. M. Hedges, J. W. Mitchell, Phil. Mag. **44,** 357 (1953).
[27] S. W. Ings, J. H. Neyhart, F. Schmidlin, J. Appl. Phys. **42**(2), 696 (1971).
[28] Z. Lui, B. Lui, J. Kong, J. Deng, J. Anal. Chem., **72,** 4707 (2000).

[29] K. Starbova, V. Mankov, N. Starbov, D. Popov, D. Nihtianova, K. Kolev, L. D. Laude, Appl. Surf. Sci. **173**, 177 (2001).

[30] E. Krumov, K. Starbova, D. Popov, G. Schlaghecken, E. W. Kreutz, accepted for publication in Proc. Six[th] Workshop "Nanostructured Materials Applications and Innovation Transfer", Nov. 2004, Sofia, Bulgaria

[31] V. Yordanova, K. Starbova, K. Kolev, L. D. Laude, Proc. Fifth Workshop "Nanostructured Materials Applications and Innovation Transfer", Nov. 2003, Sofia, Bulgaria, Nanoscienc & Nanotechnology, Eds., E. Balabanova and I. Dragieva, Heron press, p. 297.

[32] V. Yordanova et all. to be published.

[33] L. D. Laude, K. Kolev, M. Brunel, P. Deteler, Appl. Surf. Sci, **86,** 368 (1985).

[34] A. J. Pedraza, M. J. Godbole, M. J. DeSilva, D. H. Lowndes, MRS-Proc., **285** 203 (1993).